JACS
JOURNAL OF THE AMERICAN CHEMICAL SOCIETY
pubs.acs.org/JACS
Communication

Reversible Solid-State Isomerism of Azobenzene-Loaded Large-Pore Isoreticular Mg-CUK-1

Junpeng He, Kanchan Aggarwal, Naman Katyal, Shichao He, Edward Chiang, Samuel G. Dunning, Joseph E. Reynolds, III, Alexander Steiner, Graeme Henkelman,* Emily L. Que,* and Simon M. Humphrey*

Cite This: J. Am. Chem. Soc. 2020, 142, 6467−6471

ABSTRACT: A large-pore version of Mg-CUK-1, a water-stable metal−organic framework (MOF) with 1-D channels, was synthesized in basic water. Mg-CUK-1L has a BET surface area of 2896 $m^2\ g^{-1}$ and shows stark selectivity for CO_2 sorption over N_2, O_2, H_2, and CH_4. It displays reversible, multistep gated sorption of CO_2 below 0.33 atm. The dehydrated single-crystal structure of Mg-CUK-1L confirms retention of the open-channel structure. The MOF can be loaded with organic molecules by immersion in hot melts, providing single crystals suitable for X-ray diffraction. *trans*-Azobenzene fills the channels in a 2 × 2 arrangement. Solid-state UV−vis spectroscopy reveals that azobenzene molecules undergo reversible *trans*−*cis* isomerization, despite being close-packed; this surprising result is confirmed by DFT-simulated UV−vis spectra.

Hydrothermal synthesis of functional metal−organic frameworks (MOFs) using water as the only reaction medium is beneficial from an environmental perspective and provides MOFs that are inherently moisture-stable.[1] Their application as adsorbents for the capture of potable water in arid regions has been demonstrated by Yaghi and co-workers.[2] MOFs that resist hydrolytic decomposition also hold potential for applications in molecular separation/sequestration of wet feed-gas mixtures.[3]

The M-CUK-1 series of MOFs (M = Mg, Mn, Co, Ni) are prepared under sub-hydrothermal conditions (200−250 °C).[4] They are based on 2,4-pyridinedicarboxylic acid (2,4-pdc; NC_5H_3-2,4-CO_2H) and have a 1-D channel micropore structure. Since their discovery in 2007,[4b] our group and others have shown that M-CUK-1 materials act as high-capacity and highly cyclable water adsorbents for adsorption-driven chiller applications[4d] and for H_2S capture.[4e] Compared to the *d*-metal analogues, Mg-CUK-1 utilizes a nontoxic metal, can be prepared rapidly at scale (30 min) using microwave-assisted heating, has a lower gravimetric density, and has a higher thermal stability (up to 450 °C).[4a] Mg-CUK-1 selectively adsorbs *p*-isomers from crude xylenes and divinylbenzenes; single-crystal X-ray diffraction (SCXRD) also permitted valuable structural resolution of *p*-isomer-loaded materials.[4a]

Given the versatility of Mg-CUK-1, we have applied an isoreticular approach[5] to obtain a large-channel ("L") version of Mg-CUK-1, which has a greatly increased surface area and is able to adsorb azobenzene (AzB) directly from a hot melt, resulting in X-ray quality crystals. Close-packed AzB in Mg-CUK-1L surprisingly undergoes reversible *cis*−*trans* isomerism.

The ligand 4-(4-carboxyphenyl)picolinic acid ($cppH_2$; C_5H_3N-2-CO_2H-4-(C_6H_4-4-CO_2H)) has the same coordinating moieties as 2,4-pdc but is extended by an extra phenyl ring at the 4-position. $CppH_2$ was obtained in gram quantities via Suzuki coupling followed by saponification of the dimethyl ester (Supporting Information). Precipitation with excess HCl yielded $cppH_2$ as the pyridinium hydrochloride salt. Co-dissolution of $cppH_2$·HCl with 1.5 equiv of $Mg(NO_3)_2$ in water containing 3 equiv of KOH resulted in an opaque white slurry, which was heated at 240 °C, yielding colorless crystalline rods of the target MOF.

Mg-CUK-1L ($[Mg_3(\mu_3\text{-}OH)_2(cpp)_2]\cdot nH_2O$) is isoreticular with the M-CUK-1 materials and crystallizes in the same monoclinic space group ($C2/c$; Z = 4). The asymmetric unit contains one complete cpp^{2-} ligand bound to two crystallographically unique Mg(II) centers (Figure 1A). The Mg(II) coordination modes include a five-membered *N*,*C*-chelate (N1−Mg1−O1; Figure 1A) that allows cpp^{2-} to act as a linear linker akin to 4,4′-biphenyl, which yielded isoreticular versions of MOF-5.[6] However, unlike the IRMOFs, the asymmetry of cpp^{2-} results in the channel walls of Mg-CUK-1L having a double-walled structure (Figure 1B). In the original M-CUK-1 series, these structural aspects were shown to impart enhanced mechanical and chemical stability.[4]

Mg-CUK-1L has accessible channel openings of 17.3 × 13.7 Å. Compared to Mg-CUK-1 (10.0 × 9.5 Å), the channels have a 2.5× greater cross-sectional area (237 vs 95 $Å^2$; Figure 1C). The VOID utility in *Platon*[7] predicts an accessible volume of 2708 $Å^3$ $cell^{-1}$, representing 56% of the cell volume. Thermogravimetric analysis (TGA) of as-synthesized Mg-

Received: December 29, 2019
Published: March 18, 2020

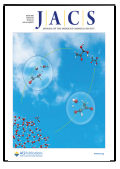

https://dx.doi.org/10.1021/jacs.9b13793
J. Am. Chem. Soc. 2020, 142, 6467−6471

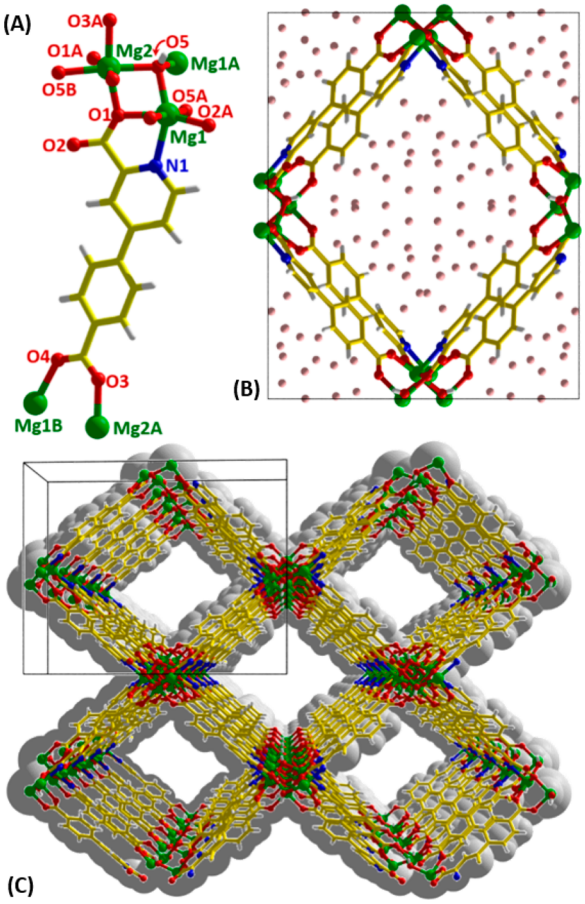

Figure 1. (A) Asymmetric unit of Mg-CUK-1L. (B) Unit cell viewed in the crystallographic *ac*-plane with solvent O atoms drawn in pink. (C) Extended view of CUK-1L showing 1-D channels; space filling model is shown in gray.

CUK-1L revealed a mass loss of 18 wt % below 60 °C (Figure S1). Comparison to a predehydrated sample indicates that H_2O undergoes dynamic exchange with ambient moisture (Figure S1, inset). The unusually low dehydration temperature is indicative of hydrophobic microchannels. Cpp^{2-} is more hydrophobic than pdc^{2-}, and the total amount of H_2O removed from Mg-CUK-1L was slightly less than for Mg-CUK-1. Between 65 and 480 °C Mg-CUK-1L lost no further mass (Figure S1); the large window of thermal stability is due to the highly electrostatic nature of Mg^{2+}−O bonds. The TGA-derived mass loss corresponds to n = 7.3 H_2O. Combustion microanalysis was in close agreement, yielding n = 7.1. Solvent O atoms (Figure 1B) were also directly located in the electron difference map, yielding n = 9.5.

Attempts were made to dehydrate a single crystal of Mg-CUK-1L *in situ* on the diffractometer by increasing the temperature of the N_2 cryostream. This method provided the dehydrated structures of the original M-CUK-1 materials, but single crystals of Mg-CUK-1L fractured upon cooling. Instead, Mg-CUK-1L crystals were predehydrated at 80 °C under vacuum and subsequently used to collect SCXRD data for the dehydrated phase (Figure 2A and Supporting Information). This confirmed that Mg-CUK-1L resisted pore collapse upon dehydration; the material shows a concertina distortion in the crystallographic *ab*-plane compared to the fully hydrated structure (dimensions = 18.1 × 12.8 Å; Figures 2, S4, and Table S1), facilitated by changes in the Mg−O bond angles.

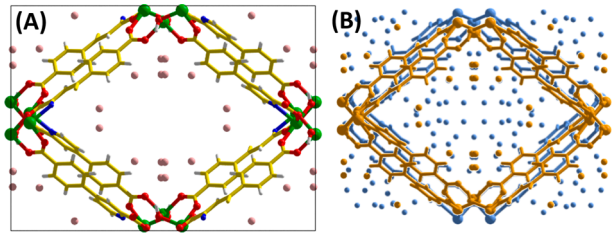

Figure 2. (A) Unit cell of dehydrated Mg-CUK-1L. (B) Superimposition of unit cells for the hydrated (blue) and dehydrated (orange) crystal structures.

The cpp^{2-} ligand also offers greater solid-state flexibility compared with the parent CUK-1 series, based on rotation between the pyridyl and phenyl rings within the channel walls (dihedral angle change = +3.1°; from 28.5° to 31.6°). In line with the hygroscopic nature of Mg-CUK-1L, trace H_2O was always found in the channels upon crystal transfer to the diffractometer, corresponding to n = 1.25; 1/4-occupancy O atoms were located only near the channel walls.

The porosity of Mg-CUK-1L was assessed by collection of adsorption−desorption isotherms between 0.02 and 0.95 atm. Crystalline samples were activated at 100 °C under vacuum overnight, and powder X-ray diffraction analysis (PXRD) confirmed that the bulk structure was retained upon activation and re-exposure to water (Figures S2 and S3). Mg-CUK-1L showed a clear sorption selectivity for CO_2 over all other gases studied (Figure 3). The maximum measured adsorption

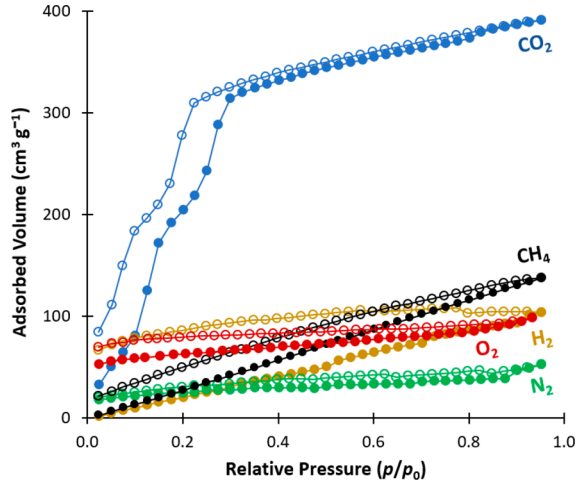

Figure 3. Adsorption−desorption isotherms for gases in Mg-CUK-1L: N_2, O_2, and H_2 at 77 K, CH_4 and CO_2 at 196 K; closed circles = adsorption, open circles = desorption.

capacity for CO_2 was 17.5 mmol g^{-1} at 196 K, corresponding to 56.6 wt %. The estimated BET surface area of Mg-CUK-1L based on CO_2 adsorption data was 2896 m^2 g^{-1}. The uptake of other gases was lower: 6.15 (CH_4; 196 K), 4.64 (H_2; 77 K), 4.23 (O_2; 77 K), and 2.37 mmol g^{-1} (N_2; 77 K). At p/p_0 = 0.4, the molar sorption selectivity for CO_2/N_2 is 8.1 and that for CO_2/O_2 is 4.7. While the latter gases showed normal type-I sorption behavior, CO_2 displayed a multistep adsorption−desorption process with a pronounced hysteresis (Figure 3; blue data). At p/p_0 = 0.02−0.33 the adsorption of CO_2 showed two distinct steps prior to saturation. The desorption hysteresis mirrored the adsorption steps, with a remanence of ca. 0.10.

https://dx.doi.org/10.1021/jacs.9b13793
J. Am. Chem. Soc. 2020, 142, 6467−6471

This type of stepped sorption behavior has been observed in MOFs with larger, meso-sized pores[8] and is commonly attributed to "gating effects", whereby a framework undergoes dynamic distortion upon loading and unloading.[9] Long and co-workers recently exploited gated CH_4 sorption in a MOF to counteract the normal thermodynamic processes, thus obtaining a larger working capacity.[10] The SCXRD structure of the dehydrated Mg-CUK-1L phase (Figure 2) indicates that a similar dynamic channel breathing effect is at play. *In situ* PXRD studies conducted at 0, 0.18, and 0.45 atm CO_2 loading (corresponding to the fully evacuated structure, before the onset of the first gating step, and at the onset of saturation, respectively) confirmed that the bulk material remained crystalline at each stage with a PXRD pattern corresponding to the fully dehydrated phase. However, upon exposure of the CO_2-loaded material to humid air for 1 h, the PXRD pattern corresponding to the fully hydrated material was recovered (Figure S4).

In an attempt to exploit the internal surface area of Mg-CUK-1L, we next studied the adsorption of larger liquid and solid hydrocarbons. Mg-CUK-1 was able to selectively adsorb *p*-xylene and *p*-divinylbenzene over mixtures of other isomers because the *o*- and *m*-isomers have larger critical diameters.[4a] The significantly larger channel openings in Mg-CUK-1L should permit entry of the larger isomers. Immersion of dehydrated crystals in *o*-xylene resulted in new high-angle reflections in the PXRD pattern (Figure S4). SCXRD analysis revealed that the channels were filled with *o*-xylene (Figure S5 and Table S1). Mg-CUK-1L⊂3(*o*-xylene) retained the same space group as the dehydrated material, and *o*-xylene molecules were packed based on host–guest π–π interactions, as well as short guest–guest CH–π contacts (Figure S5).

On the basis of this encouraging result, we explored the application of Mg-CUK-1L as a host for the capture and crystallographic determination of larger organic molecules. Fujita and Yaghi have demonstrated absolute configurational resolution of chiral organic molecules constrained inside MOF micropores.[11] There is also interest in the isolation of photoisomerizable molecules inside MOFs to probe their properties in the solid state. Ruschewitz used MIL-68 to adsorb azobenzene ($(C_6H_5N)_2$) from vapor, but only achieved 30% loading.[12] Zhou reported a MOF with azo linkages in the framework that underwent reversible *trans*–*cis* inversion upon irradiation.[13] Heinke later reported loading of AzB into HKUST-1 from ethanol, but this method did not produce crystals suitable for SCXRD.[14]

The robustness of Mg-CUK-1L enabled us to directly load AzB in Mg-CUK-1L by heating dehydrated crystals in a neat AzB melt at 80 °C, without losing crystallinity. The structure of Mg-CUK-1L⊂2AzB was solved in the triclinic space group, $P\bar{1}$ (Z = 2; Figures S5, S6 and Table S1). AzB molecules adopt thermodynamically favored *trans* configurations, and the C–N=N–C bond angles are unremarkable (Figure 4). Given the aromatic apolar nature of AzB, the closest host–guest interactions are formed with the aromatic moieties of the channel walls.[4a,d] The AzB molecules are closely packed in a 2 × 2 end-to-end arrangement (Figure 4B), with no free space remaining in the channels (Figure 4C).

Next, we assessed if photoisomerization to the *cis* form was hindered in the solid state. UV–vis spectra of hydrated Mg-CUK-1L revealed no absorption bands between 300 and 800 nm and a strong band below 250 nm corresponding to MOF-based metal–ligand charge transfer. Irradiation of the same

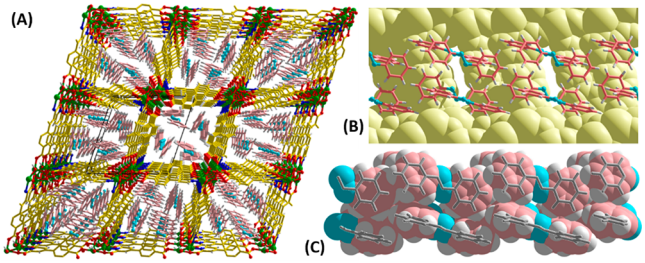

Figure 4. (A) Packing view of Mg-CUK-1L⊂2AzB in the *bc*-plane; AB molecules are drawn in pink (C) and cyan (N). (B) Cross-sectional view of a single AB-loaded channel. (C) Space-filling representation of AB molecules with the host framework removed, showing close packing of AB molecule aligned in end-to-end fashion.

sample at 320 or 460 nm for 60 s resulted in no spectral changes (Figure S7). In contrast, the UV–vis spectrum of the AzB-loaded material showed two characteristic absorbances at ca. 317.5 and 439 nm, corresponding to $\pi \rightarrow \pi^*$ and $n \rightarrow \pi^*$ transitions of AzB, respectively (Figures S8 and S9).[15] Irradiation of Mg-CUK-1L⊂2AzB at 320 nm and collection of absorbance spectra at regular intervals revealed significant diminishment of the band at 317 nm after <30 s, accompanied by an increase in the band at ca. 439 nm due to *cis*-AzB (Figures 5A and S11). The observed "soft crystalline",[16] flexible nature of Mg-CUK-1L allows the framework to accommodate the *trans*-to-*cis* conversion. Isomerization back to the *trans* state was achieved by irradiation at 460 nm for 30 s; the process was repeated over multiple cycles without loss of

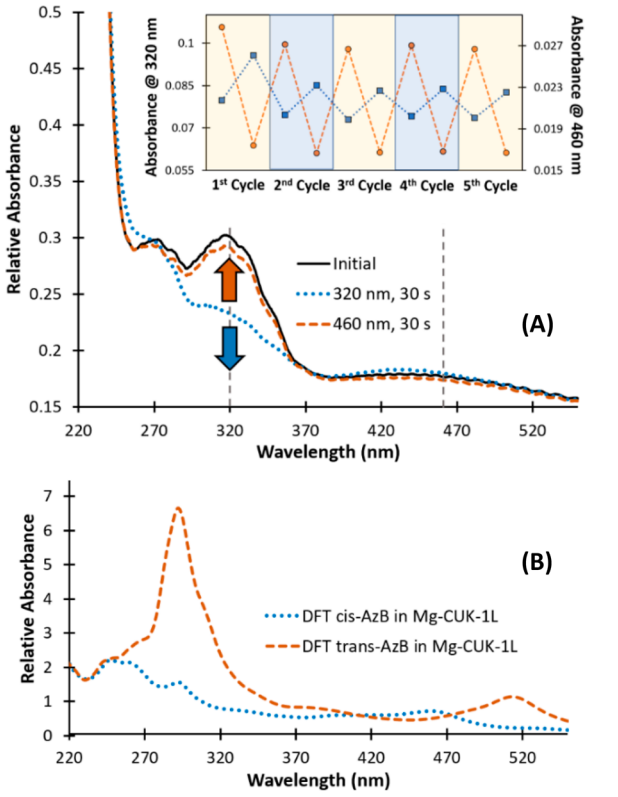

Figure 5. (A) *In situ* UV–vis spectra for Mg-CUK-1L⊂2AB showing fast and reversible loss of the *trans*-N_2 absorption at ca. 320 nm. Inset: Relative absorbances at 320 and 460 nm upon cycling. (B) DFT-calculated absorbance spectra for Mg-CUK-1L loaded with *cis*- and *trans*-AzB.

https://dx.doi.org/10.1021/jacs.9b13793
J. Am. Chem. Soc. 2020, 142, 6467–6471

integrated intensity, indicating full reversibility (Figure 5A; inset).

To further understand the *trans*−*cis* photoisomerization and to determine the origin of the loss of UV−vis response between 310 and 320 nm, DFT calculations were performed to model the optical transitions (Supporting Information). The calculated UV−vis spectra for *cis*- and *trans*-AzB molecules loaded in Mg-CUK-1L are in close agreement with the experimental observations (Figure 5B). DFT of the *trans*-AzB-loaded MOF predicted a characteristic absorption band at 295 nm that was diminished for *cis*-AzB, in line with the experimental findings. Independent UV−vis spectra calculated for isolated AzB molecules in both configurations (Figure S12) showed a strong response at 315 nm for *trans*-AzB corresponding to a $\pi \rightarrow \pi^*$ transition; the same response was weak for *cis*-AzB.

The measured rate of thermal *cis*-to-*trans* relaxation of Mg-CUK-1L⊂2AzB after irradiation at 320 nm at 298 K in the dark was slow ($t_{1/2}$ = 6.6 h; Figure S13). This enabled PXRD studies of the *cis* form immediately after irradiation at 320 nm, which revealed retention of crystallinity but no distinguishable differences in the bulk diffraction compared to the *trans* form. Furthermore, the simulated PXRD pattern for the *cis*-AzB form obtained from DFT studies is in excellent agreement (Figure S14). This is reasonable since the major reflections are due to the (ordered) host framework atoms.

Together with the DFT-predicted single-crystal structure of *cis*-AzB molecules in Mg-CUK-1L (Figure S15), it is apparent that *trans*-AzB molecules undergo reversible photoisomerization within the Mg-CUK-1L channels. Further studies using this material in water sorption and the sorption of chiral molecules are currently under way in our lab.

■ ASSOCIATED CONTENT

Supporting Information

The Supporting Information is available free of charge at https://pubs.acs.org/doi/10.1021/jacs.9b13793.

Experimental procedures and spectral data (PDF)
Crystallographic data (CIF)
Crystallographic data (CIF)
Crystallographic data (CIF)
Crystallographic data (CIF)

■ AUTHOR INFORMATION

Corresponding Authors

Emily L. Que − *Department of Chemistry, University of Texas at Austin, Austin, Texas 78712, United States;* orcid.org/0000-0001-6604-3052; Email: emilyque@cm.utexas.edu

Graeme Henkelman − *Department of Chemistry, University of Texas at Austin, Austin, Texas 78712, United States;* orcid.org/0000-0002-0336-7153; Email: henkelman@utexas.edu

Simon M. Humphrey − *Department of Chemistry, University of Texas at Austin, Austin, Texas 78712, United States;* orcid.org/0000-0001-5379-4623; Email: smh@cm.utexas.edu

Authors

Junpeng He − *Department of Chemistry, University of Texas at Austin, Austin, Texas 78712, United States*

Kanchan Aggarwal − *Department of Chemistry, University of Texas at Austin, Austin, Texas 78712, United States*

Naman Katyal − *Department of Chemistry, University of Texas at Austin, Austin, Texas 78712, United States*

Shichao He − *Department of Chemistry, University of Texas at Austin, Austin, Texas 78712, United States*

Edward Chiang − *Department of Chemistry, University of Texas at Austin, Austin, Texas 78712, United States*

Samuel G. Dunning − *Department of Chemistry, University of Texas at Austin, Austin, Texas 78712, United States*

Joseph E. Reynolds, III − *Department of Chemistry, University of Texas at Austin, Austin, Texas 78712, United States*

Alexander Steiner − *Department of Chemistry, University of Liverpool, Liverpool L69 7ZD, U.K.;* orcid.org/0000-0002-4315-6123

Complete contact information is available at: https://pubs.acs.org/10.1021/jacs.9b13793

Notes

The authors declare no competing financial interest.

CCDC numbers 1965418−1965421 contain the CIF data for structures.

■ ACKNOWLEDGMENTS

The authors thank Dr. Vince M. Lynch for X-ray assistance, the Texas Advanced Computing Centre (TACC) for computational resources, the Welch Foundation (F-1738, S.M.H.; F-1883, E.L.Q.; F-1841, G.H.), and ConTex for funding.

■ REFERENCES

(1) (a) Nandasiri, M. I.; Jambovane, S. R.; McGrail, B. P.; Schaef, H. T.; Nune, S. K. Adsorption, separation, and catalytic properties of densified metal-organic frameworks. *Coord. Chem. Rev.* **2016**, *311*, 38−52. (b) Chen, C.; Jiang, Q.; Xu, H.; Lin, Z. Highly efficient synthesis of a moisture-stable nitrogen-abundant metal-organic framework (MOF) for large-scale CO_2 capture. *Ind. Eng. Chem. Res.* **2019**, *58*, 1773−1777.

(2) Kim, H.; Yang, S.; Rao, S. R.; Narayanan, S.; Kapustin, E. A.; Furukawa, H.; Umans, A. S.; Yaghi, O. M.; Wang, E. N. Water harvesting from air with metal-organic frameworks powered by natural sunlight. *Science* **2017**, *356*, 430−434.

(3) (a) Borjigin, T.; Sun, F.; Zhang, J.; Cai, K.; Ren, H.; Zhu, G. A microporous metal-organic framework with high stability for GC separation of alcohols from water. *Chem. Commun.* **2012**, *48*, 7613−7615. (b) Zhang, H.; Xiao, R.; Song, M.; Shen, D.; Liu, J. Hydrogen production from bio-oil by chemical looping reforming - Characteristics of the synthesized metal organic frameworks for CO_2 removal. *J. Therm. Anal. Calorim.* **2014**, *115*, 1921−1927. (c) Wang, C.; Liu, X.; Demir, N. K.; Chen, J. P.; Li, K. Applications of water stable metal-organic frameworks. *Chem. Soc. Rev.* **2016**, *45*, 5107−5134.

(4) (a) Saccoccia, B.; Bohnsack, A. M.; Waggoner, N. W.; Cho, K. H.; Lee, J. S.; Hong, D.; Lynch, V. M.; Chang, J.; Humphrey, S. M. Separation of *p*-divinylbenzene by selective room-temperature adsorption inside Mg-CUK-1 prepared by aqueous microwave synthesis. *Angew. Chem., Int. Ed.* **2015**, *54*, 5394−5398. (b) Humphrey, S. M.; Chang, J.-S.; Jhung, S. H.; Yoon, J. W.; Wood, P. T. Porous cobalt(II)-organic frameworks with corrugated walls: Structurally robust gas-sorption materials. *Angew. Chem., Int. Ed.* **2007**, *46*, 272−275. (c) Yoon, J. W.; Jhung, S. H.; Hwang, Y. K.; Humphrey, S. M.; Wood, P. T.; Chang, J.-S. Gas-sorption selectivity of CUK-1: a porous coordination solid made of cobalt(II) and pyridine-2,4-dicarboxylic acid. *Adv. Mater.* **2007**, *19*, 1830−1834. (d) Lee, J. S.; Yoon, J. W.; Mileo, P. G. M.; Cho, K. H.; Park, J.; Kim, K.; Kim, H.; Lange, M. F.; Kapteijn, F.; Maurin, G.; Humphrey, S. M.; Chang, J.-S. Porous metal-organic framework CUK-1 for adsorption heat allocation toward green applications of natural refrigerant water. *ACS Appl. Mater. Interfaces* **2019**, *11*, 25778−2578. (e) Sánchez-González, E.; Mileo, P. G. M.; Sagastuy-Breña, M.; Álvarez, J. R.;

Reynolds, J. E.; Villarreal, A.; Gutiérrez-Alejandre, A.; Ramírez, J.; Balmaseda, J.; González-Zamora, E.; Maurin, G.; Humphrey, S. M.; Ibarra, I. A. Highly reversible sorption of H_2S and CO_2 by an environmentally friendly Mg-based MOF. *J. Mater. Chem. A* **2018**, *6*, 16900−16909.

(5) (a) Yaghi, O. M.; Kalmutzki, M. J.; Diercks, C. S. *Introduction to Reticular Chemistry: Metal-Organic Frameworks and Covalent Organic Frameworks*; Wiley-VCH, 2019. (b) Zhao, D.; Timmons, D. J.; Yuan, D.; Zhou, H.-C. Tuning the topology and functionality of metal-organic frameworks by ligand design. *Acc. Chem. Res.* **2011**, *44*, 123−133. (c) Garibay, S. J.; Cohen, S. M. Isoreticular synthesis and modification of frameworks with the UiO-66 topology. *Chem. Commun.* **2010**, *46*, 7700−7702.

(6) Eddaoudi, M.; Kim, J.; Rosi, N.; Vodak, D.; Wachter, J.; O'Keeffe, M.; Yaghi, O. M. Systematic design of pore size and functionality in isoreticular MOFs and their application in methane storage. *Science* **2002**, *295*, 469−472.

(7) Spek, A. L. Structure validation in chemical crystallography. *Acta Crystallogr., Sect. D: Biol. Crystallogr.* **2009**, *65*, 148−155.

(8) (a) Choi, H. J.; Dincă, M.; Long, J. R. Broadly hysteretic H_2 adsorption in the microporous metal-organic framework Co(1,4-benzenedipyrazolate). *J. Am. Chem. Soc.* **2008**, *130*, 7848−7850. (b) Ravikovitch, P. I.; Domhnaill, S. C. Ó.; Neimark, A. V.; Schüth, F.; Unger, K. K. Capillary hysteresis in nanopores: theoretical and experimental studies of nitrogen adsorption on MCM-41. *Langmuir* **1995**, *11*, 4765−4772.

(9) (a) Guo, Z.; Li, G.; Zhou, L.; Su, S.; Lei, Y.; Dang, S.; Zhang, H. Magnesium-based 3D metal-organic framework exhibiting hydrogen-sorption hysteresis. *Inorg. Chem.* **2009**, *48*, 8069−8071. (b) Mulfort, K. L.; Farha, O. K.; Malliakas, C. D.; Kanatzidis, M. G.; Hupp, J. T. An interpenetrated framework material with hysteretic CO2 uptake. *Chem. - Eur. J.* **2010**, *16*, 276−281. (c) Zhong, D.; Zhang, W.; Cao, F.; Jiang, L.; Lu, T. A three-dimensional microporous metal-organic framework with large hydrogen sorption hysteresis. *Chem. Commun.* **2011**, *47*, 1204−1206.

(10) Mason, J. A.; Oktawiec, J.; Taylor, M. K.; Hudson, M. R.; Rodriguez, J.; Bachman, J. E.; Gonzalez, M. I.; Cervellino, A.; Guagliardi, A.; Brown, C. M.; Llewellyn, P. L.; Masciocchi, N.; Long, J. R. Methane storage in flexible metal-organic frameworks with intrinsic thermal management. *Nature* **2015**, *527*, 357−361.

(11) (a) Lee, S.; Kapustin, E. A.; Yaghi, O. M. Coordinative alignment of molecules in chiral metal-organic frameworks. *Science* **2016**, *353*, 808−811. (b) Yan, K.; Dubey, R.; Arai, T.; Inokuma, Y.; Fujita, M. Chiral crystalline sponges for the absolute structure determination of chiral guests. *J. Am. Chem. Soc.* **2017**, *139*, 11341−11344.

(12) Hermann, D.; Emerich, H.; Lepski, R.; Schaniel, D.; Ruschewitz, U. Metal-organic frameworks as hosts for photochromic guest molecules. *Inorg. Chem.* **2013**, *52*, 2744−2749.

(13) Park, J.; Sun, L. B.; Chen, Y. P.; Perry, Z.; Zhou, H. C. Azobenzene-functionalized metal-organic polyhedra for the optically responsive capture and release of guest molecules. *Angew. Chem., Int. Ed.* **2014**, *53*, 5842−5846.

(14) Mueller, K.; Wadhwa, J.; Malhi, S. J.; Schoettner, L.; Welle, A.; Schwartz, H.; Hermann, D.; Ruschewitz, U.; Heinke, L. Photo-switchable nanoporous films by loading azobenzene in metal-organic frameworks of type HKUST-1. *Chem. Commun.* **2017**, *53*, 8070−8073.

(15) (a) Bandara, H. M. D.; Burdette, S. C. Photoisomerization in different classes of azobenzene. *Chem. Soc. Rev.* **2012**, *41*, 1809−1825. (b) Schultz, T.; Quenneville, J.; Levine, B.; Toniolo, A.; Martínez, T. J.; Lochbrunner, S.; Schmitt, M.; Shaffer, J. P.; Zgierski, M. Z.; Stolow, A. Mechanism and dynamics of azobenzene photoisomerization. *J. Am. Chem. Soc.* **2003**, *125*, 8098−8099.

(16) Horike, S.; Shimomura, S.; Kitagawa, S. Soft porous crystals. *Nat. Chem.* **2009**, *1*, 695−704.

https://dx.doi.org/10.1021/jacs.9b13793
J. Am. Chem. Soc. 2020, 142, 6467−6471